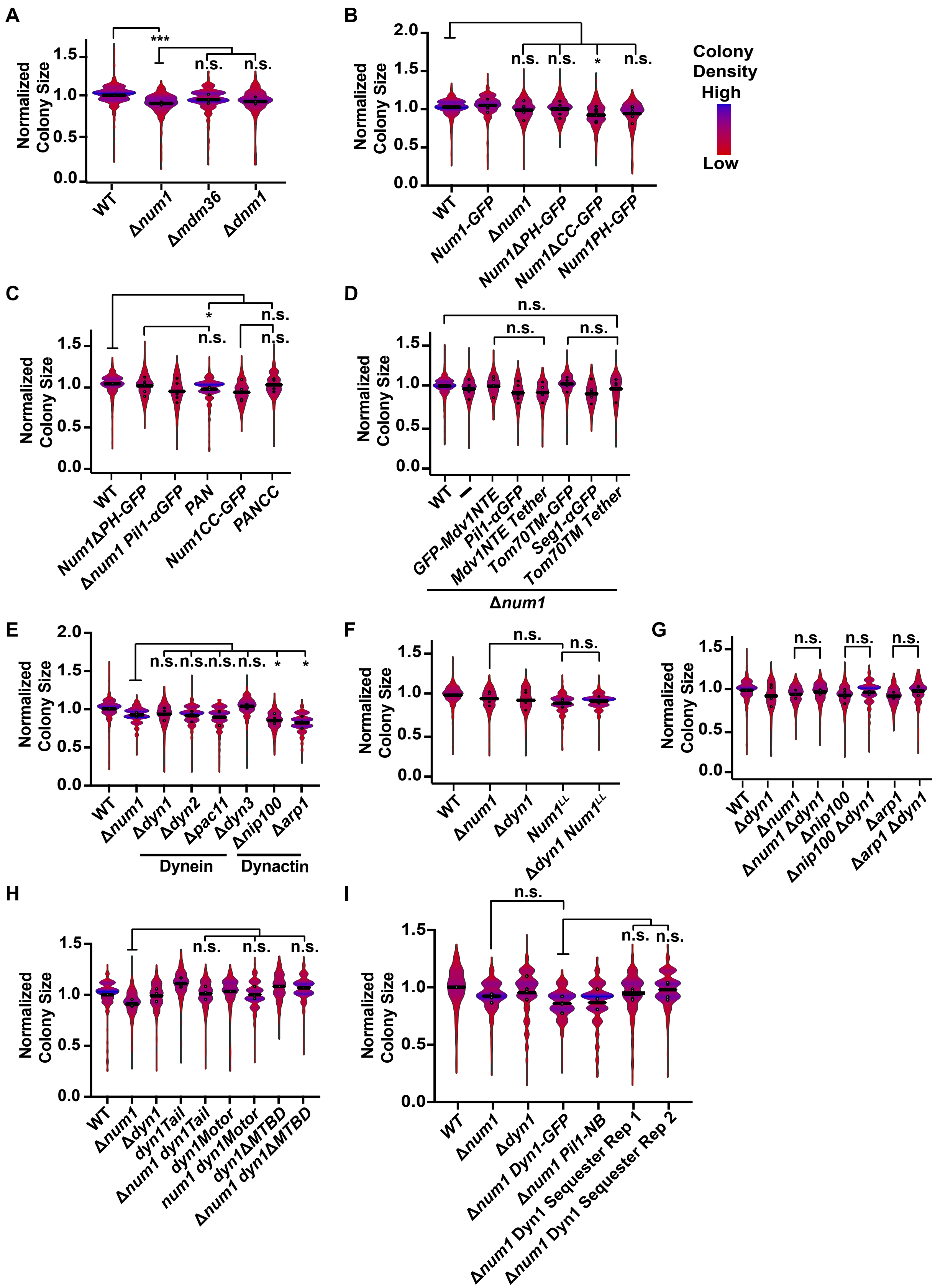

Journal of Cell Science • Supplementary information

Fig. S1. Quantification of fermentative growth for strains used in the study. (A-I) Quantification of growth at 35°C in fermentative (YPD) growth conditions as described in Figure 1E. The panels correspond to the respiratory growth data shown in the following figures: Figure 1E (A), Figure 2B (B), Figure 2F (C), Figure 3D (D), Figure 4A (E), Figure 5B (F), Figure 5D (G), Figure 5F (H), and Figure 6C. *** $p \leq 0.001$, * $p \leq 0.05$, n.s.=not significant

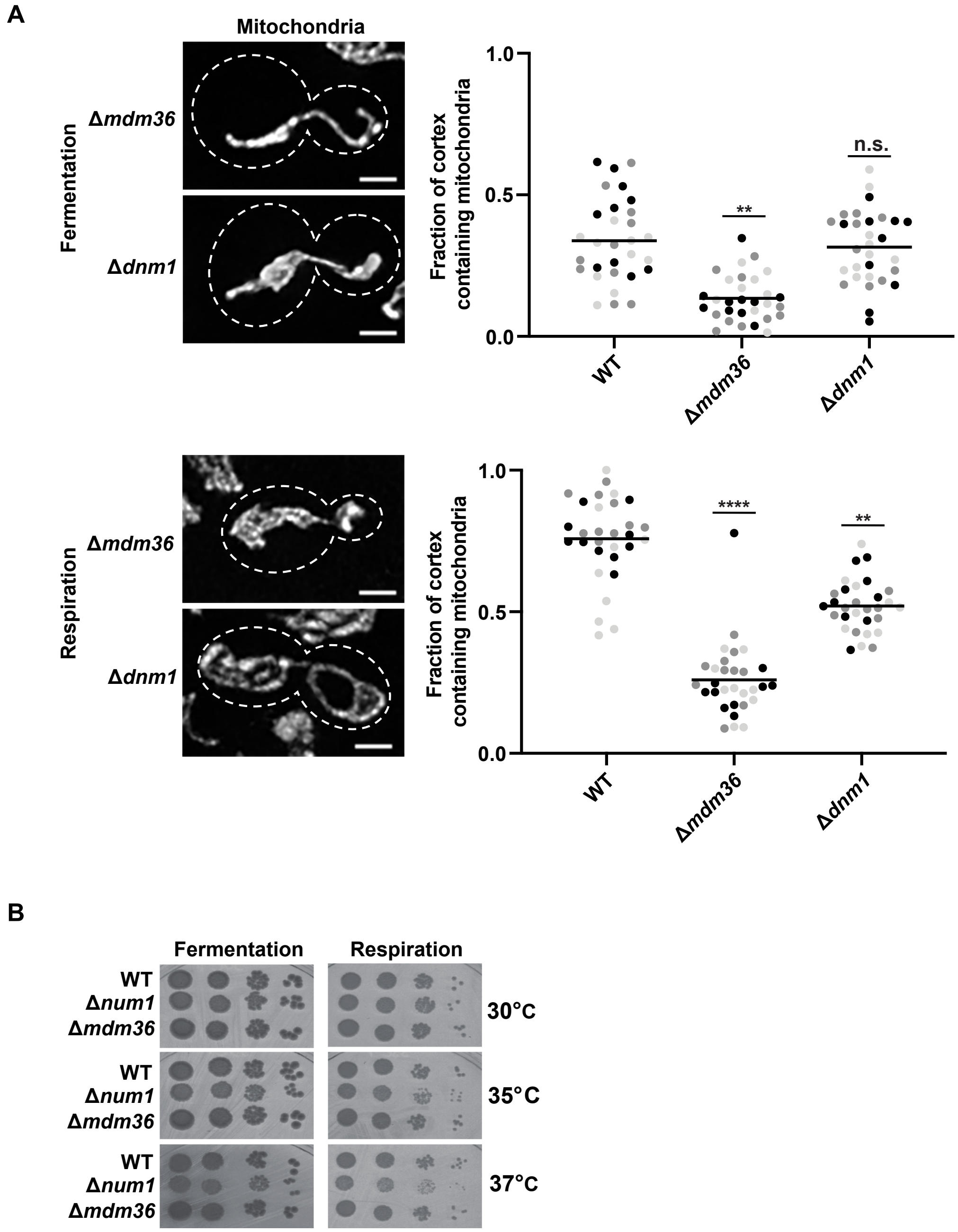

Fig. S2. Cells lacking Mdm36 or Dnm1 do not exhibit defects in respiratory growth. (A) Cells expressing mito-dsRED in WT or the absence of either Mdm36 or Dnm1 were grown in fermentative or respiratory growth conditions and analyzed by fluorescence microscopy. Whole cell, maximum intensity projections are shown. Dashed white lines denote the outline of the cell. Bar = 2 µm. The graph represents a quantification of the fraction of the cell cortex at mid-cell that is occupied by mitochondria for WT, Δ*mdm36*, and Δ*dnm1* cells expressing mito-dsRED grown in either a fermentative or respiratory growth condition, as indicated; n = 30 cells per strain from

3 independent experiments, each shown in a different color. Black line denotes grand mean. WT data are recapitulated from Fig. 1B for comparison. ****p≤0.0001, ** p≤0.01, n.s.=not significant. (B) Serial dilutions of WT, Δ*num1*, and Δ*mdm36* cells onto YPD (fermentative growth condition) or YPEG (respiratory growth condition) agar plates grown at 30°C, 35°C, 37°C, as indicated.

Journal of Cell Science • Supplementary information

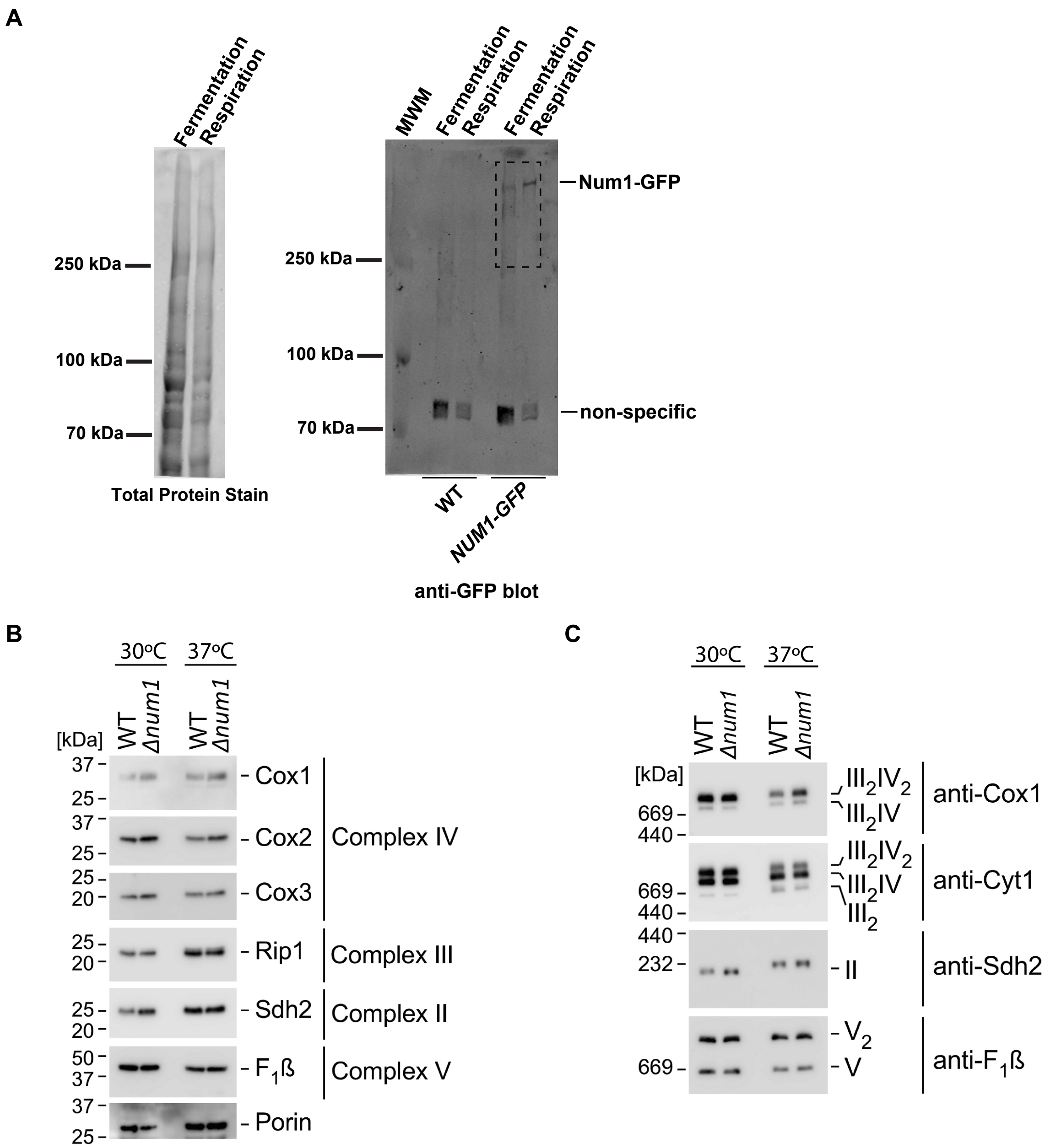

Fig. S3. Loss of Num1 function does not impact respiratory complex formation. (A) Total protein stain image (left panel) and extended anti-GFP blot (right panel) of the membrane used for the western blot shown in Figure 1C. The portion of the anti-GFP blot that is shown in Figure 1C is indicated. (B) Steady-state levels of representative subunits of respiratory Complexes IV (Cox1–Cox3), III (Rip1), II (Sdh2), and V ($F_1\beta$) along with porin (loading control) in mitochondria of WT and Δ*num1* cells grown at the indicated temperatures analyzed by SDS-PAGE immunoblotting with appropriate antibodies. Positions of molecular mass markers are indicated on the left side of the blots. (C) Blue native-PAGE immunoblotting of digitonin-solubilized mitochondrial lysates from WT and Δ*num1* cells grown at the indicated temperatures were used to examine respiratory supercomplex assembly, particularly the assembly of Complex III (anti-Cyt1 immunoblot) and Complex IV (anti-Cox1 immunoblot) into a III_2/IV_2 tetramer and a III_2/IV trimer. Positions of molecular mass markers are indicated on the left side of the blots.

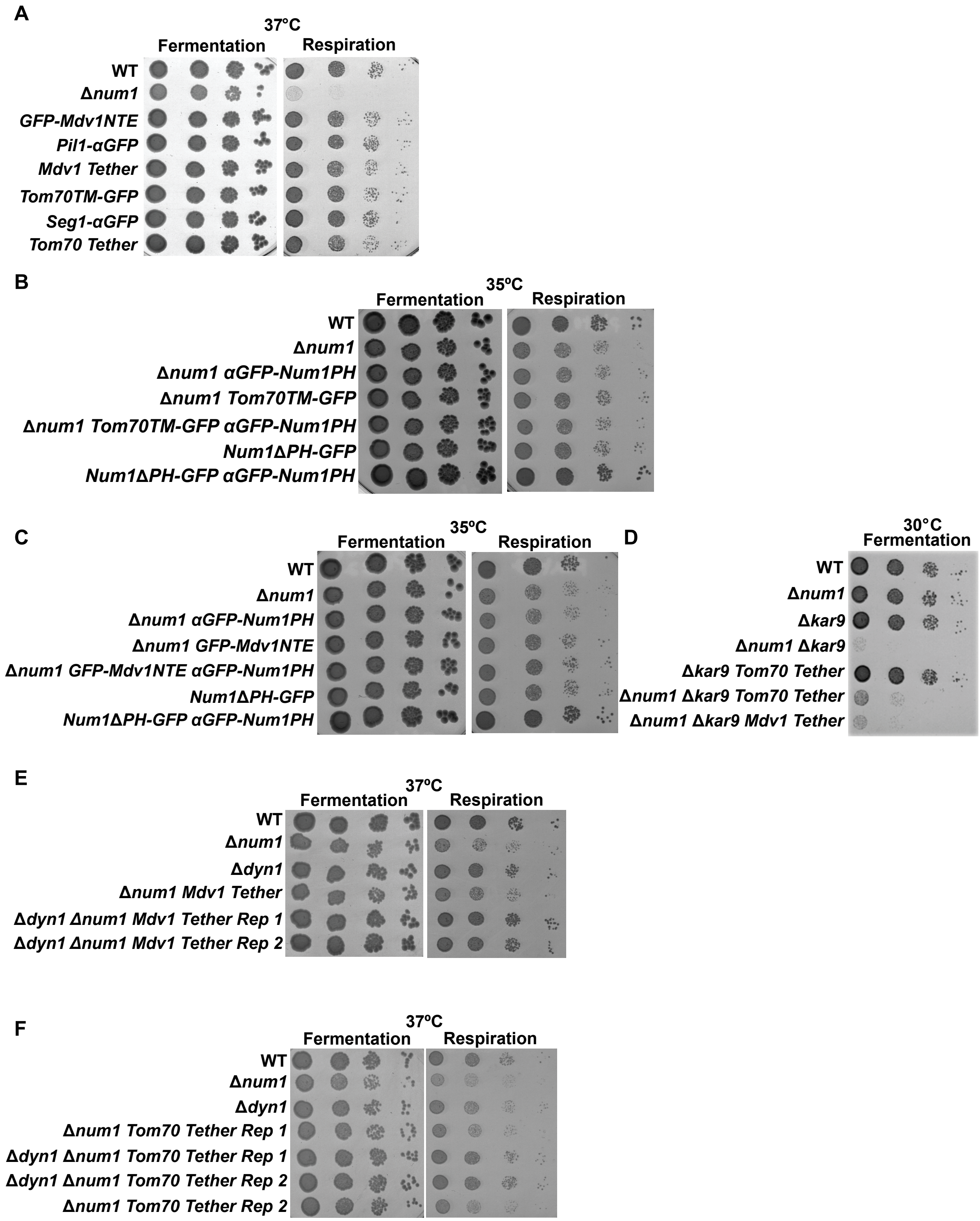

Fig. S4. Additional characterization of artificial, Num1-independent mitochondria-plasma membrane tethers. (A) Serial dilutions of WT, *Δnum1*, *GFP-MDV1NTE*, *PIL1-αGFP*, *MDV1 Tether*, *TOM70TM-GFP*, *SEG1-αGFP*, and *TOM70 Tether* onto YPD (fermentative growth condition) or YPEG (respiratory growth condition) at 37°C. (B and C) Serial dilutions of WT, Δ*num1*, Δ*num1 αGFP-Num1PH*, Δ*num1 Tom70TM-GFP* (B)/GFP-*Mdv1NTE* (C), Δ*num1 Tom70TM-GFP* (B)/GFP-*Mdv1NTE* (C) *αGFP-Num1PH*, *Num1ΔPH-GFP,* and *αGFP-Num1PH Num1ΔPH-GFP* cells were spotted onto YPD (fermentative growth condition) or YPEG (respiratory growth condition) agar plates and grown at 35°C. (D) Serial dilutions of WT, Δ*num1*, Δ*kar9*, Δ*num1* Δ*kar9*, Δ*kar9 TOM70 Tether mito-dsRED,* Δ*num1* Δ*kar9 TOM70 Tether mito-dsRED*, and Δ*num1* Δ*kar9 MDV1 Tether* onto YPD (fermentative growth condition) agar plates grown at 30°C. (E and F) Serial dilutions of WT, Δ*num1*, Δ*dyn1*, Δ*num1 Mdv1 Tether (E)/*Δ*num1 Tom70 Tether (F), and* Δ*num1* Δ*dyn1 Mdv1 Tether (E)/*Δ*num1* Δ*dyn1 Tom70 Tether (F)* onto YPD and YPEG (agar plates grown at 37°C. Rep 1 and 2 denote two independent isolates of the indicated genotype.

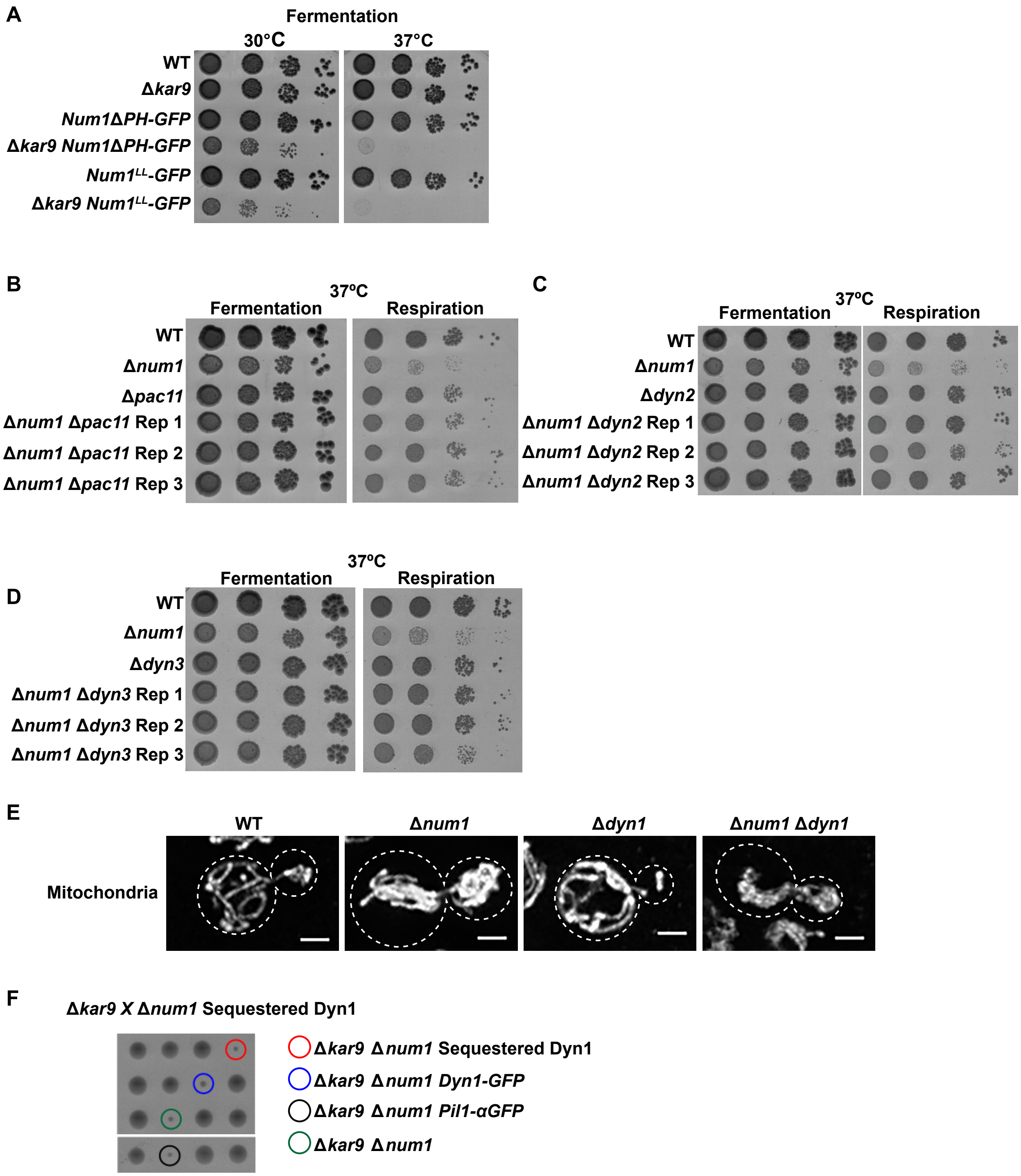

Fig. S5. Additional characterization of Num1^{LL}, dynein mutants, and eisosome-sequestered Dyn1. (A) Serial dilutions of WT, Δ*kar9*, *Num1ΔPH-GFP*, Δ*kar9 NUM1ΔPH-GFP*, *NUM1^{LL}-GFP,* and Δ*kar9 NUM1^{LL}-GFP* onto YPD (fermentative growth condition) agar plates grown at 30°C and 37°C. (B-D) To supplement the colony size assays shown in Figure 5D, serial dilutions of the indicated strains were spotted onto YPD (fermentative growth condition) or YPEG (respiratory growth condition) agar plates and grown at 37°C. Rep 1, 2 and 3 denote three independent isolates of the indicated genotype. (E) WT, Δ*num1*, Δ*dyn1*, and Δ*num1* Δ*dyn1* cells expressing mito-dsRED were grown in respiratory growth conditions and analyzed by fluorescence microscopy. Whole cell, maximum intensity projections are shown. Dashed white lines denote the outline of the cell. Bar = 2 µm. (F) Δ*kar9* Δ*num1* *PIL1-αGFP DYN1-GFP* diploid cells were sporulated, and spores from individual tetrads were arranged in a row on YPD medium. Growth on selective plates was used to score the markers for the deletions and αGFP and yEGFP fusions. The relevant genotypes are indicated.

Table S1. List of strains used in this study

Strain #	Genotype	Source
92/93	W303 (ade2–1; leu2–3; his3–11,15; trp1–1; ura3–1; can1–100)	
27/28	W303 Δnum1::HIS	Ping et al. 2016
58	W303 Δdnm1::KAN	Lackner et al. 2013
144	W303 Δdnm1::NAT Num1-yEGFP::KAN	Lackner et al. 2013
148	W303 Δmdm36::NAT Num1-yEGFP::HIS	Lackner et al. 2013
153	W303 Num1-yEGFP:KAN	Lackner et al. 2013
177	W303 Δarp1::HIS	This study
180	W303 Δnip100::HIS	This study
330/2168	W303 Δkar9::NAT	Kraft and Lackner, 2017
331	W303 Δdyn2::NAT	This study
401	W303 Δmdm36::HIS	Ping et al. 2016
647/648	W303 Δnum1::KAN	Kraft and Lackner, 2017
1184	Pil1-LaG16::CaURA3	Schmit et al. 2018
1187	W303 Num1ΔPH-yEGFP::HIS Pil1-LaG16::CaURA3	Schmit et al. 2018
1541/4876	W303 Δdyn1::NAT	Kraft and Lackner, 2017
1862	W303 Num1ΔCC-yEGFP::HIS	This study
1906	W303 Δkar9::NAT NUM1ΔPH-yEGFP::HIS	Schmit et al. 2018
2033	W303 Num1ΔPH-yEGFP::HIS	Schmit et al. 2018
2264	W303 Δnum1::HIS Pil1-LaG16::CaURA3	This study
2276	W303 Num1CC-yEGFP::HIS	Anderson et al. 2022
2278	W303 NumCC-yEGFP::HIS Pil1-LaG16::CaURA3	Anderson et al. 2022
2944	W303 Δnum1::KAN CYC1::Tom70TM-yEGFP::TRP1	This study
2974	W303 Δnum1::KAN CYC1::yEGFP-Mdv1NTE::TRP1	This study
2975	W303 Δnum1::HIS CYC1::yEGFP-Mdv1NTE::TRP1 Pil1-LaG16::CaURA3	This study
3163	W303 Δnum1::KAN Seg1-LaG16::CaURA3	This study
3179	Seg1-LaG16::CaURA3	This study
3273	W303 Δnum1::KAN CYC1::Tom70TM-yEGFP::TRP1 Seg1-LaG16::CaURA3	This study
3352	W303 Δnum1::KAN mito-dsRED::LEU/NAT	This study
3356/4957/4958/4959	W303 Num1^{LL}-yEGFP::HIS	This study
3397	W303 Δkar9::HIS Num1^{LL}-GFP::HIS	This study
3411	W303 mito Red::LEU/NAT	This study
3617	W303 Num1^{LL}-GFP::HIS mito-dsRED::LEU/NAT	This study
3619	W303 Num1-GFP::KAN mito-dsRED::LEU/NAT	This study

Journal of Cell Science • Supplementary information

3620	W303 *Num1CC-GFP::HIS Pil1-LaG16::CaURA3 mito-dsRED::LEU/NAT*	This study
3621	W303 *Num1ΔPH-GFP::HIS Pil1-LaG16::CaURA3 mito-dsRED::LEU/NAT*	This study
3703	W303 *Num1ΔPH-GFP::HIS LaG16::CaURA3-Num1PH*	This study
3705	W303 *Num1CC-GFP::HIS LaG16::CaURA3-Num1PH*	This study
3730	W303 *CYC1::Tom70TM-yEGFP::TRP1 Seg1-LaG16::CaURA3*	This study
3731	W303 *CYC1::Tom70TM-yEGFP::TRP1*	This study
3732	W303 *CYC1::yEGFP-Mdv1NTE::TRP1*	This study
3733	W303 *CYC1::yEGFP-Mdv1NTE::TRP1 Pil1-LaG16::CaURA3*	This study
3734	W303 *CYC1::Tom70TM-yEGFP::TRP1 LaG16::CaURA3-Num1PH*	This study
3737	W303 *CYC1::yEGFP-Mdv1NTE::TRP1 LaG16::CaURA3-Num1PH*	This study
3748	W303 *Δnum1::KAN LaG16::CaURA3-Num1PH*	This study
4042	W303 *Δnum1::HIS CYC1::yEGFP-Mdv1NTE::TRP1 Pil1-LaG16::CaURA3 mito-dsRED::LEU/NAT*	This study
4092	W303 *Δpac11::HIS*	This study
4094	W303 *Δnum1:::KAN CYC1::Tom70TM-yEGFP::TRP1 Seg1-LaG16::CaURA3 mito-dsRED:LEU/NAT*	This study
4106	W303 *Δnip100::HIS Num1-yEGFP::KAN mito-dsRED::LEU/NAT*	This study
4107	W303 *Δarp1::HIS Num1-yEGFP::KAN mito-dsRED::LEU/NAT*	This study
4226	W303 *Δnum1::KAN CYC1::yEGFP-Mdv1NTE::TRP1 mito-dsRED::LEU/NAT*	This study
4227	W303 *Num1CC-yEGFP::HIS mito-dsRED::LEU/NAT*	This study
4229	W303 *Δmdm36::NAT Num1-yEGFP::HIS mito-dsRED::LEU/NAT*	This study
4230	W303 *Δnum1::KAN CYC1::Tom70TM-yEGFP::TRP1 mito-dsRED::LEU/NAT*	This study
4231	W303 *Num1ΔPH-yEGFP::HIS mito-dsRED::LEU/NAT*	This study
4305/4306/4307	W303 *Δnum1::HIS Δdyn1::NAT*	This study
5560/5561/5562	W303 *Δnum1::HIS Δdyn2::NAT*	This study
4311/4312/4313	W303 *Δnum1::HIS Δpac11::HIS*	This study
4315/4316/4317	W303 *Δdyn1::NAT Δnip100::HIS*	This study
4318/4319/4320	W303 *Δdyn1::NAT Δarp1::HIS*	This study
4465	yJM1494 *dyn1ΔMTBD*(Δ3102-3225) Tub1-GFP::LEU	Estrem et al. 2017
4472	W303 *Δnum1::HIS Δdyn1::NAT mito-dsRED::LEU/NAT*	This study

4657/4658	W303 *dyn1Tail-3XFLAG::HIS*	This study
4630/5507	W303 Δ*num1::KAN dyn1Tail-3XFLAG::HIS*	This study
4843/4844	W303 *dyn1Motor-3XFLAG::HIS*	This study
4846/4847	W303 Δ*num1::KAN dyn1Motor-3XFLAG::HIS*	This study
4929/4930/4931	W303 Δ*dyn1::NAT Num1*^{LL}*-yEGFP::HIS*	This study
4963	W303 *CYC1::Tom70mito-yEGFP::TRP1 Seg1-LaG16::CaURA3* Δ*kar9::NAT mito-dsRED:LEU/NAT*	This study
4964	W303 Δ*num1:::KAN CYC1::Tom70mito-yEGFP::TRP1 Seg1-LaG16::CaURA3* Δ*kar9::NAT mito-dsRED:LEU/NAT*	This study
4965	W303 Δ*num1::HIS CYC1::yEGFP-Mdv1(1-241)::TRP1 Pil1-LaG16::CaURA3* Δ*kar9::NAT*	This study
5068	W303 Δ*dnm1::NAT Num1-yEGFP::KAN mitoRed::NAT/LEU*	This study
5104	W303 Δ*dyn1::NAT mito-dsRED::LEU/NAT*	This study
5176/5177	W303 Δnum1*::HIS Dyn1-yEGFP::KAN Pil1-LaG16::CaURA3*	This study
5184	W303 Δ*num1::KAN Dyn1-yEGFP::KAN*	This study
5354/5355	W303 Δ*dyn3::KAN*	This study
5376/5377/5407	W303 Δ*dyn3::KAN* Δ*num1::HIS*	This study
5468/5469	W303 *Num1PH-GFP::HIS*	This study
5466/5467	W303 *dyn1*Δ*MTBD-3XFLAG::HIS*	This study
5500/5501/5508	W303 Δ*num1::KAN dyn1*Δ*MTBD-3XFLAG::HIS*	This study

Table S2. List of primers used in this study

Primer #	Name	Sequence (5' → 3')
156	Arp1 F1	GCTATACCACGAATTGAGGAATTAGAAAGAAAGTTAGCCACGG ATCCCCGGGTTAATTAA
157	Arp1 R1	GCTATTTATAACAAATATGCTTGAAAAATCTAACGACTCTGTTT CGAATTCGAGCTCGTTTAAAC
163	Nip100 F1	GATTCGATCTCCATCAACCTCGCAGTACAGCCTTGGACAACGG ATCCCCGGGTTAATTAA
164	Nip100 R1	CCATTTATTTACTGTATTTGAATGTTATAGACCTGCTAGAATCA CTCAGGAATTCGAGCTCGTTTAAAC
177	Num1 F5	GACATAGAGTACCACAAAGCCGATCATTTGGCAATTTACGAGG TGACGGTGCTGGTTTA
178	Num1 R3	GATTATTATTGTTCTTAATTTACTTAGAGTTATTTAGTTTTTTTAA TCGATGAATTCGAGCTCG
270	Dyn1 F5	CGAACGTCTTCAGGCTAAAGAGGTGGCTAGCTCAACTGAACAA CTTCTTCAAGAAATGGGTGACGGTGCTGGTTTA
271	Dyn1 R3	GAATAGGCACGTCCACTGAGAAAACCGCGGACAAGCAAGACA CGCGTACCTGAAAAGGTCGATGAATTCGAGCTCG
435	Num1 aa288-303 fwd	GAAGTATTATCAAAAACAGCATACTTCCGATACTACAGTAACAT C
436	Num1 aa288-303 rev	GATGTTACTGTAGTATCGGAAGTATGCTGTTTTTGATAATACTT C
513	Num1 upstream into gene	CGAGTAAAGACGCAACGGTCAAGGCTTTCCACGAGACGTTCG AATATGTCCCACAACAACAGGCATAAAAAGAATAAC
514	Num1 end no stop	TCGTAAATTGCCAAATGATCGGCTTTGTGGTACTCTATGTC
614	Dyn1 upstream into gene	CAGAGCTTAAATTGGAAAGTACGTCAAAACGTTTTTTAGGCAAT GTGCAAGAATGAGGCAAGACTTGC
617	Dyn1 end no stop	CATTTCTTGAAGAAGTTGTTCAGTTGAGCTAGCCACCTCTTTAG CCTGAAGACGTTCG
742	Num1 upstream into aa295	CGAGTAAAGACGCAACGGTCAAGGCTTTCCACGAGACGTTCG AATATGCATACTTCCGATACTACAGTAACATCTGATCCTG
1103	5' BglII-yEGFP	GAAGATCTATGTCTAAAGGTGAAGAATTATTC
1104	3' XhoI-Mdv1 NTE 1-241	GCAGCTCGAGTCAATTTAAAAACTCTAAACTATTTACAAGAG
1449	Dyn1 Verify 7455 bp Rev	CAAATTCTCGAATTCTTAAAAGTTCC

1450	Dyn1 Verify 7300 bp Fwd	CGTCTATGTTATTGATACAAAAGTTC
1459	Pac11 F1	CAGTTGGTTAATCAACCAAAGAGGAAGAAGGATTGAAACATTAAGCGGATCCCCGGGTTAATTAA
1460	Pac11 R1	GAAATTACTCATCAGGCAATAACCTATGCTCACCCGCCTCGAAGCGGCGGAATTCGAGCTCGTTTAAAC
1723	Dyn1 aa1363 F5	CAATTTAACTTTAAATGAAATACTACTTACAAAGATTATAGAAAGAGCCCAAAAGGGTGACGGTGCTGGTTTA
1778	Dyn3 F1	CCGCAACTTGTACAAAAAGAAAAGAAGATAAAAGAATTGTATGTATTACGGATCCCCGGGTTAATTAA
1779	Dyn3 R1	CATATAAAGAGAAAAAAATTGCTCATGATAAAAGAAGTATCGCCTGCCCACTTTCGAATTCGAGCTCGTTTAAAC
1780	Dyn1 Upstream ATG into Motor Domain	CAGAGCTTAAATTGGAAAGTACGTCAAAACGTTTTTTAGGCAATGGAATTTGTTATAGAAAAGTCTCTGAACAGAATC
1838	Dyn2 NAT F1	GAAACTGGGAAACGACATAAAGAAGAGCAAATTAAAACCAAAGCTTCGTACGCTGCAGGTCG
1839	Dyn2 NAT R1	GTATAATAGTAATTGATTATCGATTAACTATTGAAGAAACACTATGTTTTCGACACTGGATGGCG
1913	Num1 Upstream into PH	GACGCAACGGTCAAGGCTTTCCACGAGACGTTCGAATATGAACGAACCAAGCATAATACC